Shear mode M3 in the first sites of ductile metallic alloys: Some considerations on the physical mechanisms leading to internal particle flows

Christine Boher, Vanessa Vidal, Elodie Cabrol, Y. Berthier, Farhad Rezai-Aria

Shear mode M3 in the first sites of ductile metallic alloys: Some considerations on the physical mechanisms leading to internal particle flows

C. Boher[a,*], V. Vidal[a], E. Cabrol[b], Y. Berthier[c], F. Rezai-Aria[a]

[a] Institut Clément Ader (ICA), Université de Toulouse, CNRS, Mines Albi, UPS, INSA, ISAE-SUPAERO, France
[b] Université de Lyon, CNRS, Ecole Nationale d'Ingénieurs de Saint-Etienne, LTDS UMR 5513, France
[c] Université de Lyon, CNRS, INSA-Lyon LaMCoS UMR5259, France

A B S T R A C T

This paper examines plastic mechanisms that lead to damage to the sub-surfaces of ductile metallic contact areas and, by extension, to the creation of wear particles. The word "damage" is used here as a generic term to designate all topological, morphological and/or microstructural modifications to the surfaces that are the consequence of interfacial shear stress under friction. During friction, the accommodation mechanisms of plastic deformation by the M3 mode in the contact area can be different, depending on the microstructures of the alloy and the first sites (bulk materials).

For example, for tempered martensitic steels under frictional stresses, plasticity strain occurs in Tribologically Transformed Surfaces (TTS) under dislocation gliding. The creation of new dislocations and the rearrangement of all these dislocations into a "bamboo"-type structure leads to a decrease in hardness, or softening of the steel.

Otherwise, depending on the stacking fault energy in alloy microstructures, plasticity may occur through mechanisms involving either perfect dislocation gliding and/or partial dislocation gliding. In addition to hardening, the mobility and morphology of dislocations are also related to stacking fault energy, which can promote phase transformation leading to shear strain in TTS. These shear strain mechanisms have a great influence on the internal flow of wear particles and on the formation of the "Third-body layers". These findings are given in a review of tribological results of measurements carried out on a wrought X38CrMoV5 grade steel and on cobalt-base thick coatings, using tribometers, under various loadings, test temperatures and sliding speeds. The cobalt-base thick coatings are deposited on steel by several processes which modify the nominal chemical composition of the cobalt alloy and make it possible to study the influence of the iron content on shear strain under friction stresses.

Keywords:
Friction
Mechanisms of plasticity
Ductile alloys
Third-Body
Shear Mode M3

1. Introduction

It has been known for many years that, under friction stresses, specific layers with more or less "amorphous" feature are observed on the sub-surfaces of ductile materials. These layers (Tribologically Transformed Surfaces (TTS) or Superficial Tribological Transformations (STT) or Mechanically Modified Superficial (MMS) structures) are the result of changes in the microstructural features, chemical composition, and mechanical and thermal properties of the ductile friction surfaces submitted to large plastic deformations under high hydrostatic pressures, even at low temperatures [1–3]. Some authors [4] consider that all metallurgical transformations within TTS are linked to the modification of mechanical and physical properties and also to the heat exchanges and/or volume variations that produce expansion or shrinkage of the sub-surface, and therefore produce internal stresses according to the direction of the transformation. TTS are often described as being sub-micrometrically structured or nano-structured, and as having epitaxial continuity with the first body (initial material). This epitaxial relationship ensures the continuity of the atomic bonds between the atoms of the substrate and those of the TTS considered as a quasi-amorphous structure [2]. Authors also observe gradients of large plastic deformations in the thickness of the friction sub-surfaces and explain that the local friction shearing stresses are responsible for extensive plastic deformation in the top of the sub-surface [5–8]. The TTS are linked to these high sub-surface plastic strains and the TTS thickness depends on both material properties and test conditions.

Under friction loadings, TTS produce wear particles from their highly-deformed sub-surfaces. These wear particles can also be highly deformed and mixed with the antagonist material. They may also produce new compounds because of atmospheric environmental effects

* Corresponding author.
E-mail address: christine.boher@mines-albi.fr (C. Boher).

such as oxidation. The size of the particles coming from these highly-deformed layers is sub-micrometric and this may be because of the plastic deformation of the grains. In the contact area, these particles can adhere to one of the antagonists and form superficial layers known as “Third-Body” layers [2] that participate in contact accommodation. The “Third-Body” can be correlated to the “Mechanically Mixed Layer” (mechanical mixing of debris and contaminants) or a “Transfer Layer” (material transferred from the counterface) as described by some authors [6,7,9,10].

The “Third-Body” concept emphasizes that particle detachment, particle flow, and particle ejection from the contact area have to be considered in order to describe wear. This concept attempts to solve friction and wear problems by considering tribological analyses of friction as a problem of “Third-Body” rheology and wear as a problem of “Third-Body” flows [2,11–13]. These analyses take into account the tribological triplet composed of the mechanisms that contain the contact, the first two bodies that form it, and the “Third-Body” that separates them. Velocity accommodation can be localized in different Sites (S:5 sites) and produced by different Modes (M:4 modes). Thus, the accommodation mechanisms combine as of one Site and one Mode to achieve the movement. More specifically, the Mode M3, also named the shear mode, is used to explain the mechanism of velocity accommodation by plastic shearing deformation.

The contribution of the TTS in the formation of the “natural Third-Body” is very important. The “Third-Body” is the result of an interaction between the first bodies (or frictional antagonists) that separates them in the contact and contributes to transmitting the load from one solid to the other. The “Third-Body” flows so as to accommodate the major part of the velocity difference between the two bodies. The wear processes governing wear particle production, the source of the “Third-Body”, can therefore be abrasion, adhesion [14,15], delamination [16] and cracking. In the tribological concept of the “Third-Body”, the accommodation sites of the TTS will be considered as the first bodies (S1 and / or S5) and the accommodation site of the transfer layers will be the S3 site [2,11].

As Berthier [2] has shown, the TTS are the responses permitting the production of the “Third-Body” with the minimum amount of surface degradation through friction. The terms most often used to describe a ductile tribological sub-surface are “plastic deformation (or plastic strain)”, “Mechanically Modified Superficial structures”, and also “cumulative plastic strain (or ratcheting)” [3,6,17]. Because these expressions imply broad physical concepts, more and more authors are investigating how to develop them in terms of physical mechanisms [18–20]. Some authors have released [21] from TTS observations of titanium alloy under fretting solicitations that one of the mechanisms of friction-induced plastic deformation may consist of an initial dislocation slip in the higher-density planes. They added that the term of "dynamic recrystallization" used to describe the formation of TTS may sometimes be inappropriate because temperatures are not high enough. TTS, they suggest, are “built” step by step, from the most distorted surface layers with the deformed grains acting as generators of overstresses on the other grains. Thus, new germination sites could appear at the interface between the matrix and the deformed grains to form the TTS.

In the case of Copper friction, Meshi et al [20] discussed dislocation features and the hardness of sub-surfaces under different conditions of friction (Elasto-hydrodynamic conditions with a low friction coefficient and boundary conditions with a high friction coefficient). Under a low friction coefficient, the formation of twin rotation boundaries and dislocation networks - due to activation of new active slip systems, during friction experiments - has been observed. Under a high friction coefficient (boundary conditions), a “drastic” transformation of dislocation features occurs. Strain localization leads to the formation of the nanocrystalline structure, while propagation of shear bands and the structural change are responsible for the grain refinement.

Authors have also observed that under friction sliding, phase transformations such as metallurgical transformations, can occur. This is known as the TRIP (TRansformation Induced by Plasticity) effect. This phenomenon is particularly notable in some austenitic stainless steels in which there are metastable phases [9,22–26]. Some coatings made of cobalt-base alloys (stellite) display martensitic transformation in the sub-layers of the contact surface under friction experiments, i.e. deformation leading to transformation of the cobalt alloy from a metastable Face Centered Cubic (FCC) microstructure to a Hexagonal Closed Pack (HCP) microstructure [27–30]. Authors attribute the galling resistance of thick cobalt-base alloy coatings to a low stacking fault energy, which contributes to the deformation-induced martensitic phase transformation under friction solicitations. For low stacking fault energies, the distance between two partial dislocations increases and the cross slip of the perfect dislocation becomes more difficult; in this case, FCC to HCP crystallographic transformation can occur. This leads to an enhanced work-hardening rate, which would be beneficial because it would prevent plastic deformation of the asperities, and thus improves adhesion resistance [27,31]. The addition of alloying elements, in the Co-Base material, leads to a change in the level of the stacking fault energy. In particular, the iron-element increases this energy and thus enlarges the stability area of the metastable Face Centered Cubic microstructure [30].

The purposes of this article are to investigate some mechanisms of plasticity in Tribologically Transformed Surfaces (TTS), to define the consequences of an accumulation of plastic deformation in the material’s response in terms of the “Third-Body” concept and to express the shear Mode M3, in physical terms. The scope of these considerations is based on different ductile alloys: a dual tempered martensitic steel and cobalt-base alloy coatings highlight their differences in terms of the physical mechanisms of accommodation of the plastic deformation in the tribological sub-surface.

2. Material and methods

The dual-tempered martensitic steel (X38CrMoV5 steel) and the cobalt-base alloy (coating of stellite 21 grade) are commonly used in forging tools. X38CrMoV5 steel is used as a bulk material in forging dies and stellite 21 is used as a thick (> 1 mm) wear-resistant coating of forging-die surfaces [30–35]. In these experiments, stellite 21 coatings on 40NiCrMo18 steel substrate were applied by two processes (a MIG welding process and a LASER cladding) in order to assess the influence of chemical composition on the plastic deformation of cobalt-base coatings (differences due to the process parameters) [30].

X38CrMoV5 dual-tempered martensitic steel is used in hot-working tools. The prior austenitic grains have a 20 μm mean size. In the grains, the martensitic laths (0.3–2 μm thick and 5–15 μm long) are decorated by different types of precipitates which are identified as lengthened $(Fe,Cr)_3C$ carbides, spherical MC carbides and angular M_7C_3 carbides. Diameters of spherical and angular particles range from 0.05 to 0.5 μm and from a few nanometers to 0.1 μm, respectively [36].

The knowledge of the mechanical behavior of the steel is important for the following considerations. The mechanical properties drop considerably beyond the tempering temperatures and this decrease can be attributed to an over-tempering. With regard to tensile ductility, the value of the maximum elongation never exceeds 25% regardless of the temperature of the test. Tensile tests show the sensitivity of X38CrMoV5 steel to temperature but also show that this type of stress is not representative of what would be observed in friction loading. In contrast, the torsion ductility values are totally different from the tensile values. For torsion test, at the rupture, the plastic deformation ε_p of the X38CrMoV5 steel can reach more than 60% at room temperature and more than 700% at 640 °C [33]. This confirms its high ductility under torsional stresses and the level of plastic strain is close to that observed at the contact sub-surface of the X38CrMoV5 tribological samples with the high deformation of the martensitic laths.

The mechanical behavior of the X38CrMoV5 steel under cyclic

solicitations (isothermal and non-isothermal fatigue) is characterized by a continuous softening. This is explained as a change in its microstructure, caused by the redistribution and the morphology of dislocations (decrease in dislocation density) and by carbides coalescence [33,37]. The type of cycle imposed (displacement or load control) to achieve a certain level of plastic deformation also influences the cyclic response of the X38CrMoV5 steel. When the test is stress-controlled with a loading that is not purely alternative, a cumulative plastic strain (ratcheting) is observed [37]. This property will be used to explain the tribological behavior of X38CrMoV5 steel.

As regards the cobalt-base (stellite 21 grade) coatings, the filler material is a stellite 21 wire for the MIG process while a stellite 21 powder is used for the LASER process. The initial chemical compositions of the wire and powder are very similar, with a very low iron content (< mass 3,5%).

The microstructure of the thick coatings is dendritic and characterized by columnar grains perpendicular to the substrate surface (Fig. 6-a) [30]. The carbides are precipitated into inter-dendritic spaces. The input energies differ in these two processes, generating more or less fine microstructures and thus different initial hardnesses. The dilution rates of the iron-element from the substrate steel into the whole thickness of the coating are also different. Thus the MIG coating with the highest process energy leads to a rather coarse microstructure, a lower hardness and an iron-element content higher than that of the LASER coating. In the friction contact areas of the stellite 21 coatings using the MIG process, the iron content is around mass 37% against mass 0.5% with the LASER process (mean values obtained by Energy Dispersive X-ray Spectroscopy analyses in cross-sections of the coatings on 120 µm x 25 µm areas).

As previously mentioned, for cobalt-base alloys, the thermodynamically stable structure is Hexagonal Closed Pack (HCP). For Co-base coatings, because the processes induce high local temperature and rapid cooling rates, the cobalt-base coating microstructure is constituted of a metastable Face Centered Cubic (FCC) phase. Therefore under specific mechanical solicitations, martensitic transformation from FCC to HCP becomes possible, independently of a thermal source. However, the greater the iron dilution is in the coating, the higher the iron content will be, making the martensitic transformation of FCC to HCP more difficult. Because of the dilution of the substrate during the coating production, the iron-content modifies the initial hardness: the greater the iron content, the lower the hardness.

The tribological devices used were a pin-on-disc tribometer and a ring-on-disc tribometer. These two devices have been extensively presented in previous research works [30,32,33].

The tribological behavior of X38CrMoV5 steel was studied under the pin-on-disc tribometer (Table 1) and the stellite coating behavior was studied under the ring-on-disc tribometer (Table 2). In all the friction experiments, the pin was made of X38CrMoV5 steel and the ring of stellite 21 grade coatings on steel.

3. Results and discussion

3.1. Tribologically Transformed Surfaces and wear particle shape

3.1.1. TTS and wear particle shape of a dual-tempered martensitic steel

For a large number of friction experiments on the dual-tempered martensitic steel (X38CrMoV5 steel), SEM observations of the wear surfaces of the pins were made on cross-sectioned samples cut parallel to the friction direction. The outcome was similar for all observations (Fig. 1): the microstructural observations showed that regardless of the test duration, the test temperature or the contact geometry of the pin, a sheared plastically-deformed depth of martensite laths was observed. The martensitic microstructure in the form of laths represents an excellent morphological marker, which makes it possible to observe and partially quantify the plastic flow under the friction surface. The thickness of the sheared plastically-deformed area was in the same

Table 1
Tribological parameters for X38CrMoV5 steel tests.

Contact geometry	Friction surface design of the pin	Disc grade	Pin grade	Normal load (N)	Sliding speed (mm/s)	Disc nominal temperature (°C)	Time test (s)
pin-on-disc	Flat contact or Hemispherical contact Flat contact	C18(AISI 1018)	X38CrMoV5(AISI H11)	20, 40 40	130 300 10	20, 200, 500, 700, 900 900	120, 300, 3600 5, 20, 120

Table 2
Tribological parameters for Stellite 21 grade coating tests.

Contact geometry	Tribological conditions	Disc grade	Ring grade	Normal load (N)	Sliding speed (mm/s)	Disc nominal temperature (°C)	Time test (s)
Ring on disc	Very severe	Stellite 21coating (MIG process)	Stellite 21 coating (MIG process)	5000 & 3000	70	Room temperature	7320
	Severe	Inconel 718	Stellite 21 coating (MIG process)	5000	80	Room temperature	1800
	Close to industrial forging conditions		Stellite 21 coating (MIG or LASER processes)	8000	5	Room and high temperatures	800

order of magnitude (< 10 µm) for all the tribological test parameters used. It varied in the range of 2–5 µm and tended to an asymptote when the sliding distance increased [34].

Nano-hardness measurements were performed to determine the hardness level in the TTS (Fig. 2). During indentation, the set-up parameters were the penetration depth of the Berkovich-type indenter and the loading speed. In this case, the depth was set at 1 µm, which gave an indent diagonal of about 7 µm, with the loading speed was equal to 800 mN/min. The measurements (Fig. 2) showed a decrease in the pin-surface hardness.

In the plastically-deformed areas of the pins, an equivalent shear plastic strain was calculated using the slope-change measurement method [19,39] (Fig. 3). It can reach a value superior to 800% in the upper layer (less than 2 µm thick). The distribution of the thickness affected by the plastic deformation showed an evolution that was in conformity with the literature, in which such a gradient is already mentioned for some ductile alloys [38].

The plastically sheared area at the extreme surface of the micrographs in Fig. 1 can be considered, in terms of definition, as TTS. It corresponds to a zone that is strongly plastically deformed with a nanometric crystalline structure rather than amorphous one. This upper layer can also be identified as the "Debris Process Zone" [34] or, in other words, the "wear-particles emission area". In Fig. 1-b, the onset of partial emission of wear particles in the TTS is observed and the wear particle is 0.2–0.4 µm thick.

It was mentioned previously that torsion (shear) ductility is about 724% at 640 °C. By plotting this value in the power-law equation of the evolution of the equivalent shear plastic strain (%) versus depth from the friction surface (Fig. 3), 724% of plastic strain corresponds to a depth of 0.43 µm, i.e. 8% of the apparent plastic-deformation thickness. Considering this result, the thickness of the wear-particle emission area (upper layer of the TTS) can be calculated and identified as less than 0.5 µm thick.

In the Third-Body concept, this area is defined as a First Body and named Site 1 (S1 for the pin). The velocity accommodation is produced

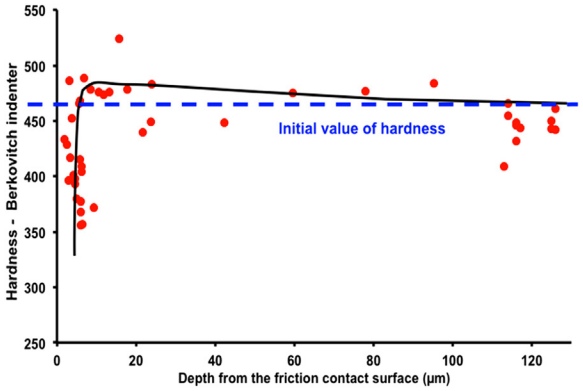

Fig. 2. Evolution of the nano-hardness from the friction contact surface towards the core of the X38CrMoV5 steel pin after friction experiment of 120 s duration.

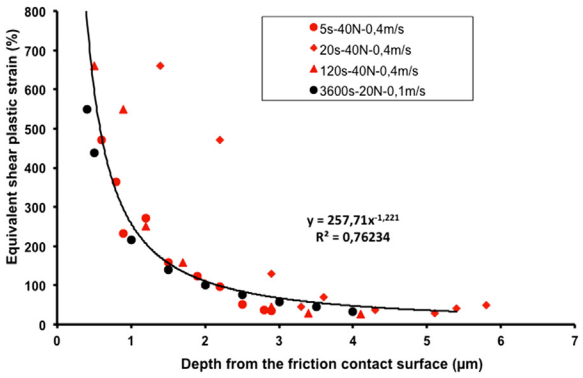

Fig. 3. Evolution of the equivalent shear plastic strain (%) from the friction contact surface towards the core of the X38CrMoV5 steel pins (plane pin geometry).

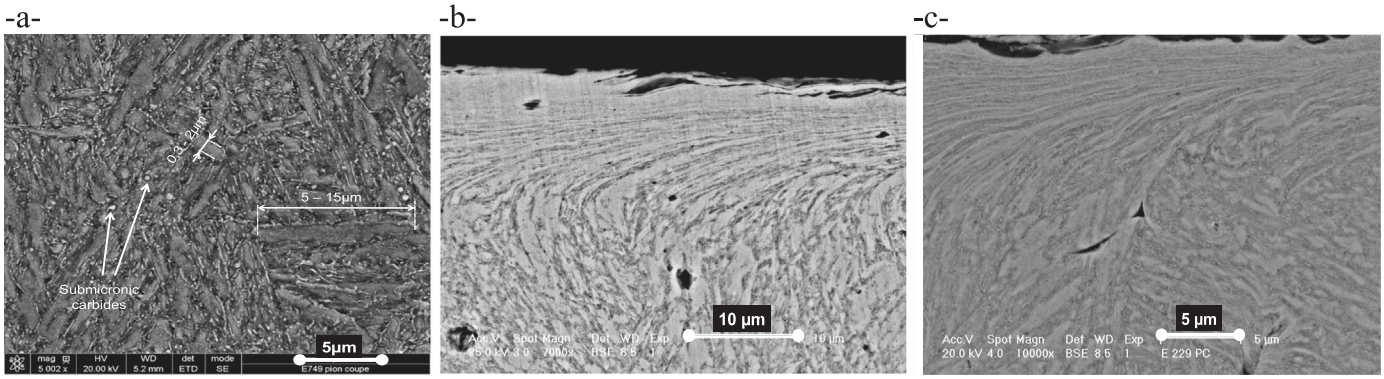

Fig. 1. Cross-section observations of X38CrMoV5 steel pins [33] a- Microstructure of X38CrMoV5 dual tempered martensitic steel before friction experiment, b- Start of partial emission of wear particle (friction experiment with disc nominal temperature: 200 °C- 40N- 130 mm/s), c- Large plastic flow (friction experiment with disc nominal temperature: 700 °C- 40N- 130 mm/s).

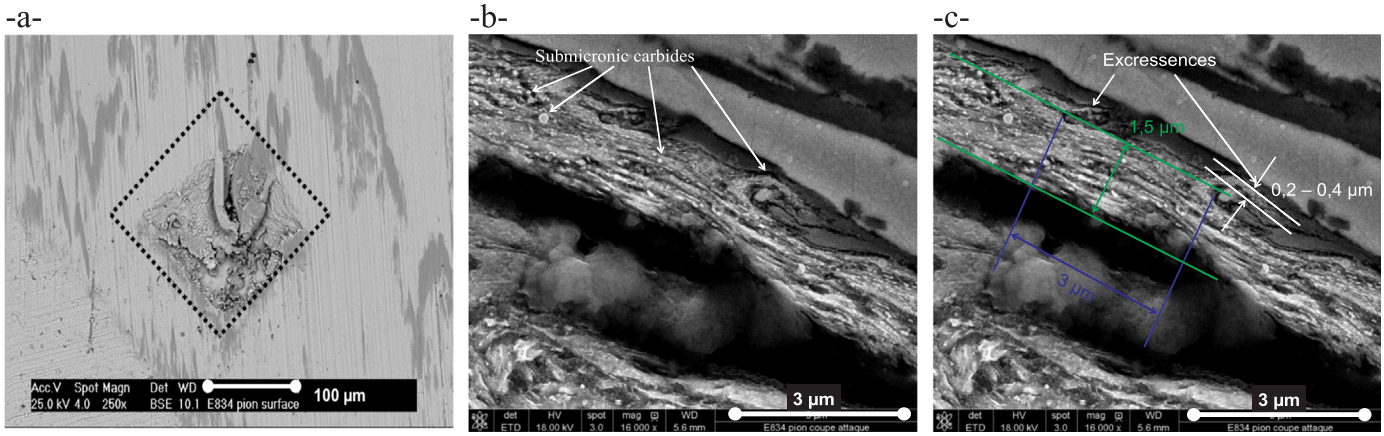

Fig. 4. Observations of micro-strips in "artificial" particle trap (plane pin, 40 N-0.40 m/s, nominal disc temperature 900 °C) [35] -a- Surface observation of micro-strips in one "artificial" particle trap, -*b*- Cross section observation of a micro-strip extruded after 10 s (length ≈ 100 µm), -c- Micro-strip with excrescences.

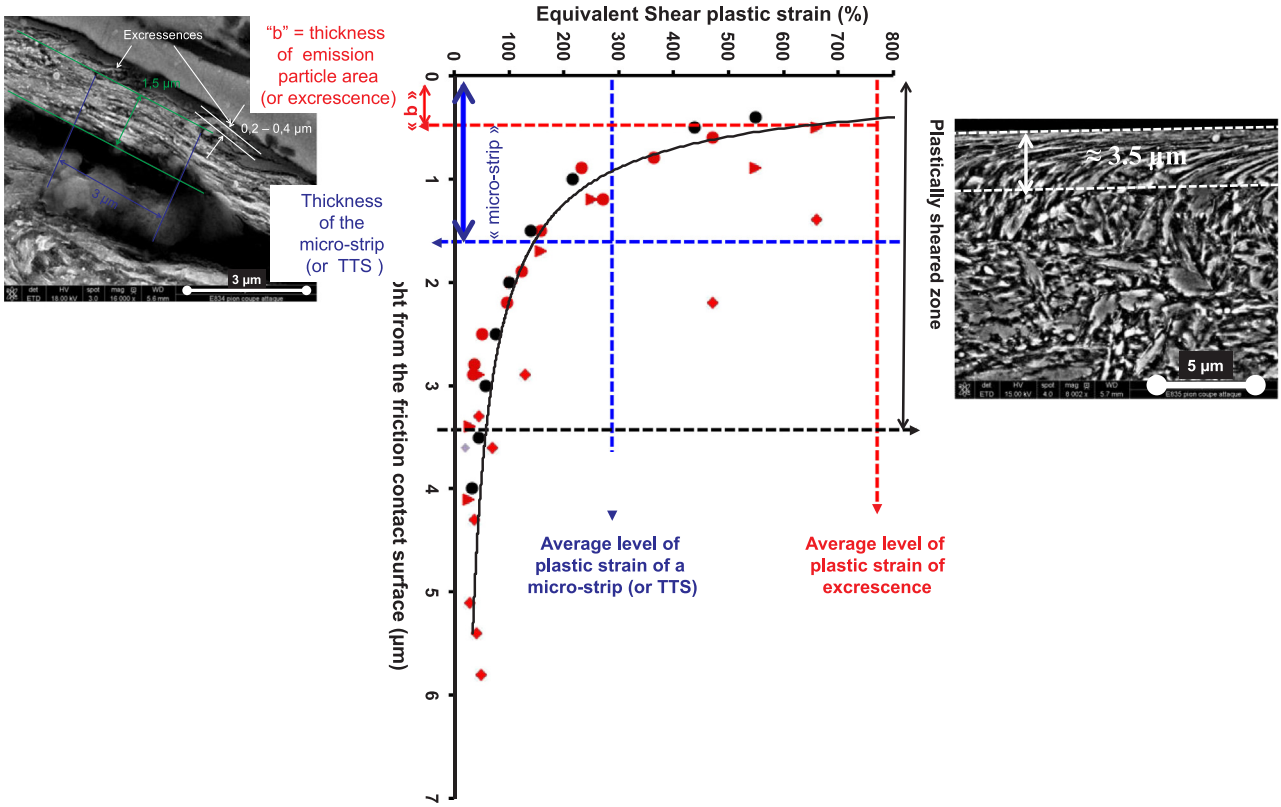

Fig. 5. Identification of the different shear plastic zones in the plastic deformation gradient areas (TTS) of the X38CrMoV5 steel pins (plane pin geometry).

via M3 Mode, which refers to the shearing mode. So, the combination of S1M3 (one Site "S" and one Mode "M") is the accommodating mechanism that enables sliding (sliding friction in the investigated cases).

The shape of the wear particle was identified using "artificial" particle traps (made via Vickers indentation) on the surface of X38CrMoV5 steel pins [35]. These traps help the observation of the Third-Body flows particularly under very short tribological test durations (5 s or 10 s). The traps have the feature of naturally extruding the plastic flow zones of the pin surface. Micro-strips on the surface of traps were observed (Fig. 4-a). The length of the micro-strip can reach 100 µm while the thickness is less than 2 micrometers (Fig. 4-a). The micro-strips consist of several martensite laths, which are plastically deformed under the shear stresses (Fig. 4-b). We can count about ten laths in a thickness of 1.5 µm, which reduces the lath dimension to a value between 0.10 and 0.2 µm (1 µm is the initial average value of lath thickness). The micro-strip could correspond to the TTS. The micro-strips also presented excrescences on their surfaces, indicating inter-lath shearing (Fig. 4-c). The distance between excrescences was about 3 µm and the thickness of these excrescences was in the range of 0.2–0.4 µm.

These excrescences are therefore made of one or two plastically deformed martensite laths and could correspond to the wear-particle emission area with regard to Fig. 1-b. The thickness of the excrescences could correspond to those of the upper layer of the TTS, because the metallic wear particles, achieved by ruptures in the wear-particle emission area, have the same shape with these excrescences. With regard to the evolution of the shearing deformation, the excrescences corresponded to the thickness of the martensitic laths that reached the critical strain (> 700%, i.e. shearing deformation) by cumulative cyclic plastic deformation (ratcheting) and can be related to the last step of

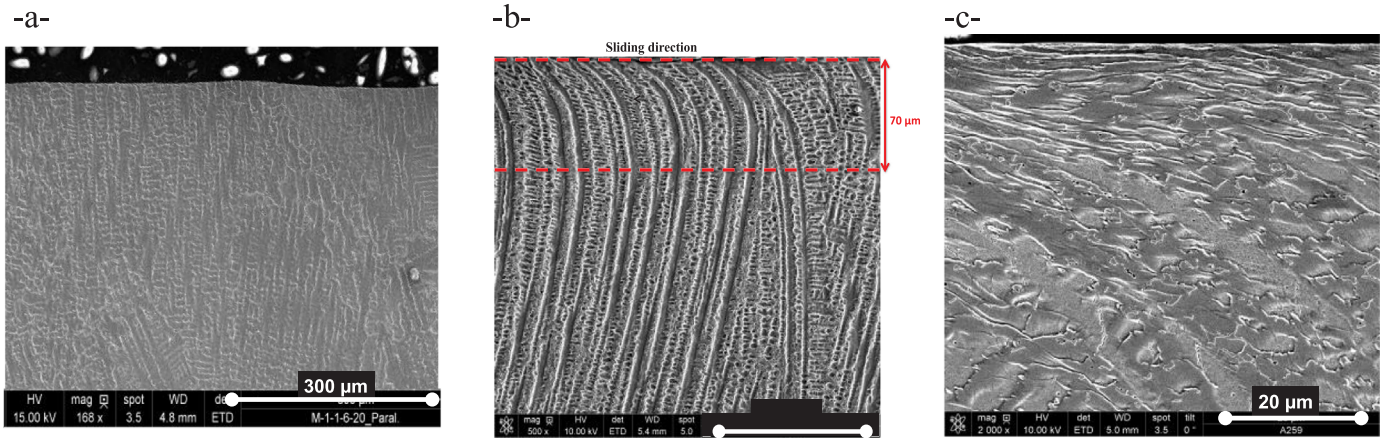

Fig. 6. Observation of plastic flow of the dendrites for cobalt-base coatings, in the TTS, before and after friction experiments, -a- Example of a microstructure of cobalt-base coating (MIG stellite) before friction experiment, -*b*- LASER stellite coating, friction parameters: 8000 N, 5 mm/s, 450 °C, -c- LASER stellite coating, friction parameters: 8000 N, 5 mm/s, 20 °C.

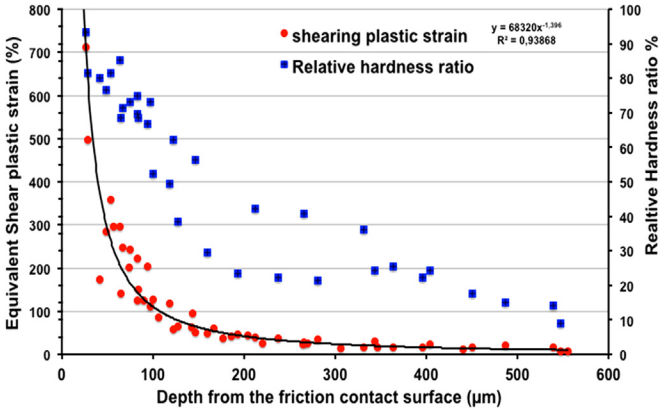

Fig. 7. Calculated shearing plastic rates (%) and evolution of the relative hardness ratios (%) of MIG cobalt-base alloy coatings (very severe tribological conditions).

plastic deformation before rupture (that is to say at thickness "b") [34]. These considerations are summarized in Fig. 5. When the wear particle was outside of the TTS (out of the friction contact), the same mechanism occurred in the sub-layers of the TTS.

The contact accommodation is therefore (S1M3)M2 with M2, the rupture Mode. The metallic wear particles can be introduced into the contact and may participate in the formation of a Third-Body (Site S3).

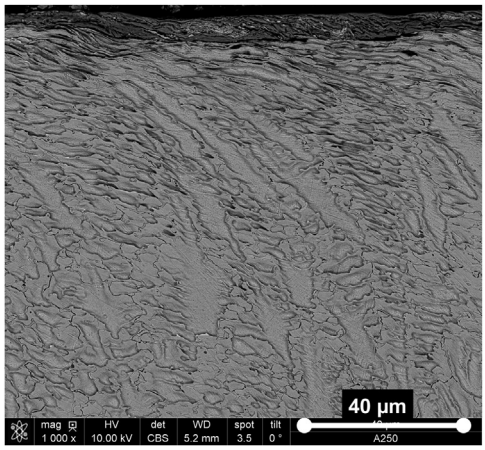

Fig. 9. SEM observation of a mechanically mixed layer (MML) or transfer layer above tribologically transformed surfaces (TTS) for LASER cobalt-base coating (Table 2: severe tribological conditions).

Their evolution in the contact will depend on the thermal and mechanical conditions of the friction experiment. If the test is carried out at high temperatures, these metallic particles oxidize to become an oxidized Third-Body, which will be plastically deformed in the friction contact and will have its own Modes of friction contact accommodations (S3Mx with Mx = M2 rupture and/or M3 predominantly shear).

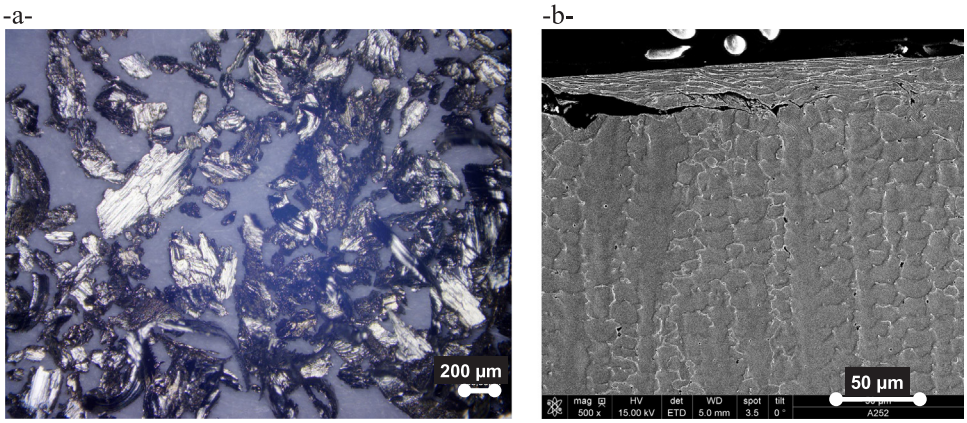

Fig. 8. Large wear particle from the Tribologically Transformed Surfaces (TTS) in cobalt-base coatings (Table 2: very severe tribological conditions), -a- Large "free" wear particle (optical microscope), -*b*- Large wear particle partially detached from the Tribologically Transformed Surfaces (TTS).

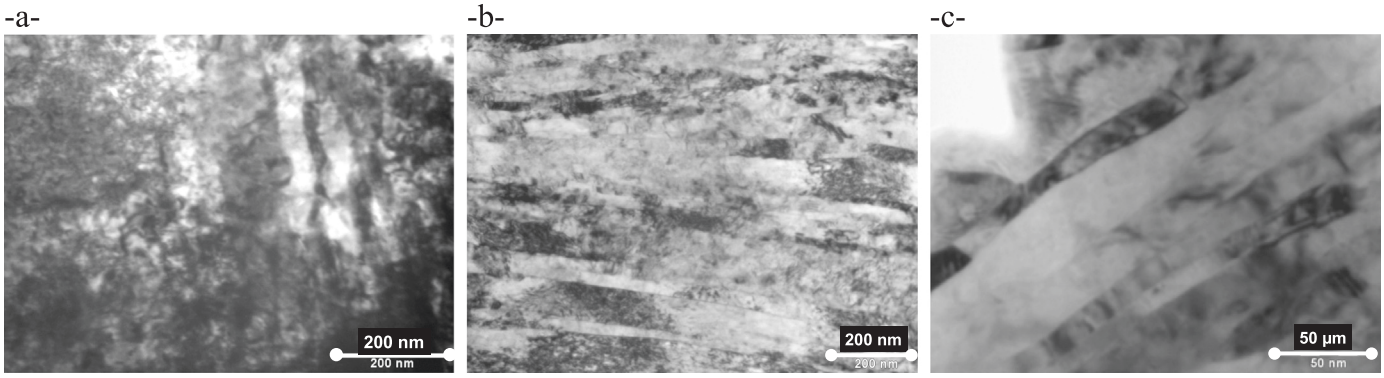

Fig. 10. TEM observations of the TTS for X38CrMoV5 pin (20N-0.13 m/s, 3600s), -a- TEM micrograph, 2.5 µm below the friction surface: very high dislocation density, -*b*- TEM micrograph, 0.5 µm below the surface: grains/sub-grain alignment with a slight decrease of dislocation density, -c- TEM micrograph, 0.5 µm below the friction surface: sub-grains alignment /low dislocation density (nanostructuration).

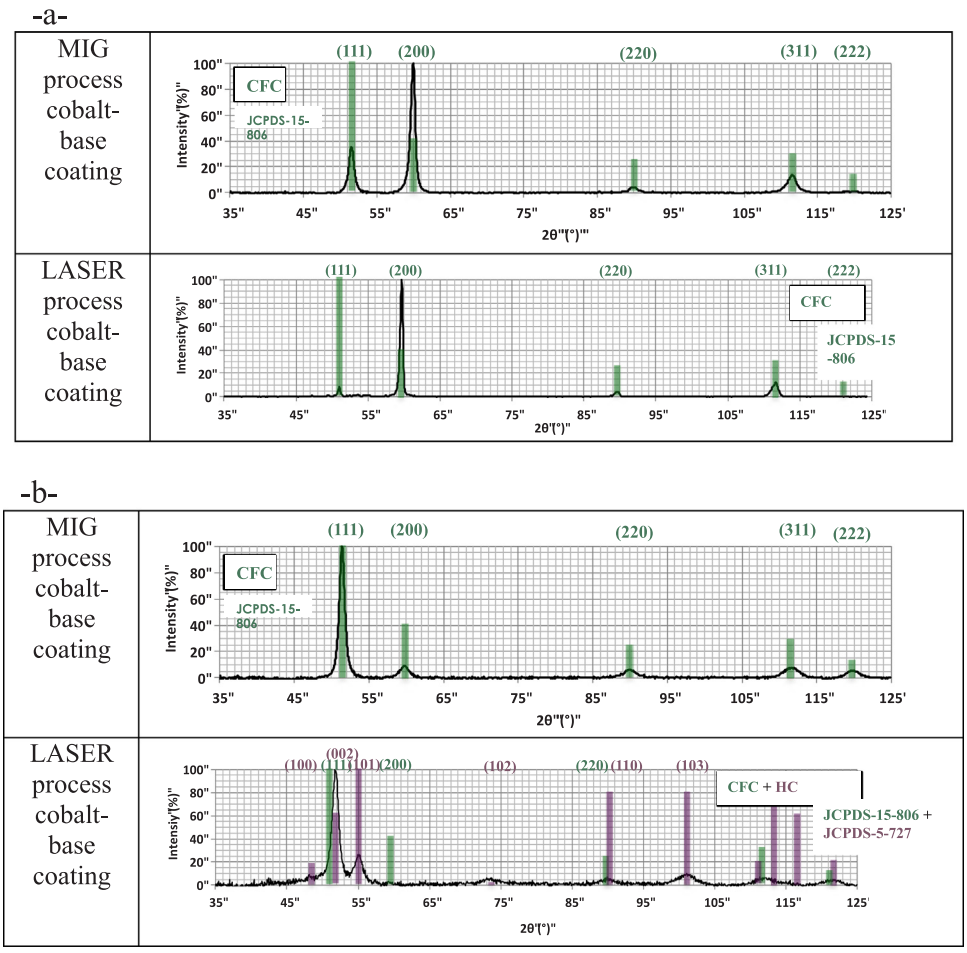

Fig. 11. XRD analyses of the upper layers of the TTS for cobalt-base alloy coatings (MIG and LASER processes), -a-Before friction experiment, -b-After friction experiment (parameters close to industrial forging conditions - Table 2) [30].

These phenomena occur during the very early instants of friction experiments (the first 5 s according to our tests).

The spherical sub-micrometric carbides (secondary carbides) are still present in these micro-strips and have not been sheared. They flow during the plastic deformation. Thus, they modify the lath plastic flow and could be responsible for inter-lath debonding and thus be micro-crack initiation sites that propagate through the laths, favoring the emission of the metallic wear particle (Fig. 4-b).

3.1.2. TTS and wear particle shape of the cobalt-base alloy (stellite 21 coating)

SEM cross-section investigations parallel to the direction of friction surfaces also showed that the plastic flow of the dendrites occurs regardless of the tribological test parameters (load, speed, test temperature) (Fig. 6-b). In the TTS, the flow gradient is significant up to a thickness of 200 µm and at higher magnification it was observed, for the first 70 µm, that the plastic flow is fully assumed by the dendritic matrix, and the inter-dendritic carbides are wholly or partially cracked. The carbides are "embedded" in the plastic flow and become markers of

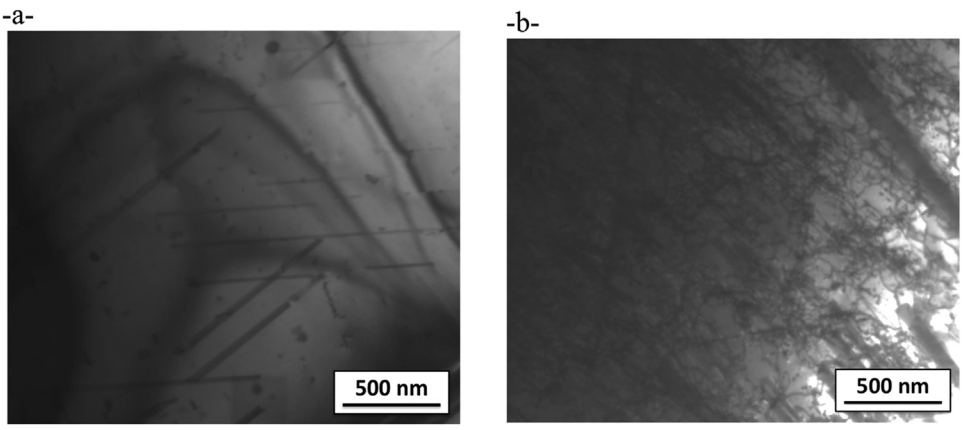

Fig. 12. STEM observations (Bright Field) of the microstructure of a MIG cobalt-base coating, -a- Before friction experiment with presence of stacking faults, -b- After friction experiment with high dislocation entanglements.

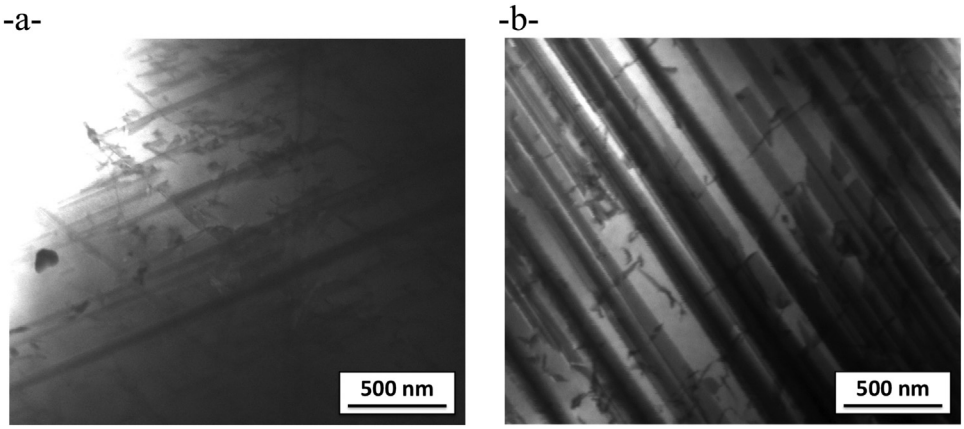

Fig. 13. STEM observations (Bright Field) of the microstructure of a LASER cobalt-base coating, -a- Before friction experiment, -b- After friction experiment with the increase of stacking defects (black stripes) and very few dislocations (500 N- 80 mm/s-1800 s).

plastic shear deformation (Fig. 6-b and c). According to our investigations, the plastic flow of the matrix seems to be minimized because of these carbide networks. One might call this a mechanical "girdle" of the microstructure.

As in the previous experiments, an equivalent shear plastic strain in the coating thickness was calculated using the slope-change measurement method. With the example of MIG stellite coatings under tribological conditions, the equivalent shear plastic strain was less than for X38CrMoV5 steel but it could still reach values superior to 300% in the upper layers of the TTS for rather short time tests and more than 600% for a "long-time" test (severe tribological conditions).

Before any friction experiments were carried out, hardness measurements highlighted differences between coatings that were caused by the effects of each process. The hardness is impacted by the finesse of the microstructure and also by the iron content, due to the dilution of the substrate during the process. The higher the process energy is, the lower is the hardness. Thus, for the MIG coatings, because of a high content of iron (37% mass), they have a lower hardness (350 $HV_{0.3}$) in comparison to the LASER coatings (430 $HV_{0.3}$).

After friction experiments, a significant increase in the hardness in the sheared areas (Fig. 7) was observed. In the upper part of the plastically-deformed zone, regardless of the coating initial hardness, the final hardness reached a maximum value around 700$HV_{0.3}$. A relationship between the evolution of the equivalent shear plastic strain and the relative hardness ratio (%) (Eq. (1)) was plotted for a "long-term" test for MIG Stellite coating (which is more appropriate for this measurement) (Fig. 7). The variation in sheared plastic deformation follows a similar pattern to that of the relative hardness ratio. From 100 µm up to the upper layers of the TTS, the relative hardness ratio exceeds 50%. For shear plastic strain higher than the threshold strain at 400%, the relative hardness reaches an asymptotic level of 85%. Strain-hardening is so observed in the TTS zone, in particular in the top layer. The maximum relative hardness ratio (%) is about 85% for the upper layers in the MIG coating TTS and about 50% for the upper layers in the LASER coating TTS.

$$\frac{(Hspsr_{0,1} - H_{\text{core}})}{H_{\text{core}}} \quad (1)$$

Hardness H_{core} is the average hardness of the coating outside of the friction area and $H_{spsr0,1}$ is the measured hardness at the same depth of the calculated shearing plastic strain rate [30].

Because of high normal loads, a few very large, free wear particles were observed (Fig. 8-a and b) and these particles were sheared (Fig. 8-b).

In most of the tribological tests, Mechanically Mixed Layers (MML) were observed at the contact surface above the TTS. These MML can be considered as the Third-Body (named Site 3-S3 in the Third Body concept) and are the result of large deformation, attrition and compaction of wear particles coming from the TTS (from the two antagonists), which adhere to the friction contact surface. The Mechanical Mixed Layers could be similar to glazed layers and are located above the TTS (Fig. 9). As found previously, the contact accommodation therefore becomes (S1M3)M2 with M2, the rupture Mode. This mechanism implies formation of the MML leading to the formation of the Third-Body S3 which is sheared (mode M3) to accommodate the contact (S3M3).

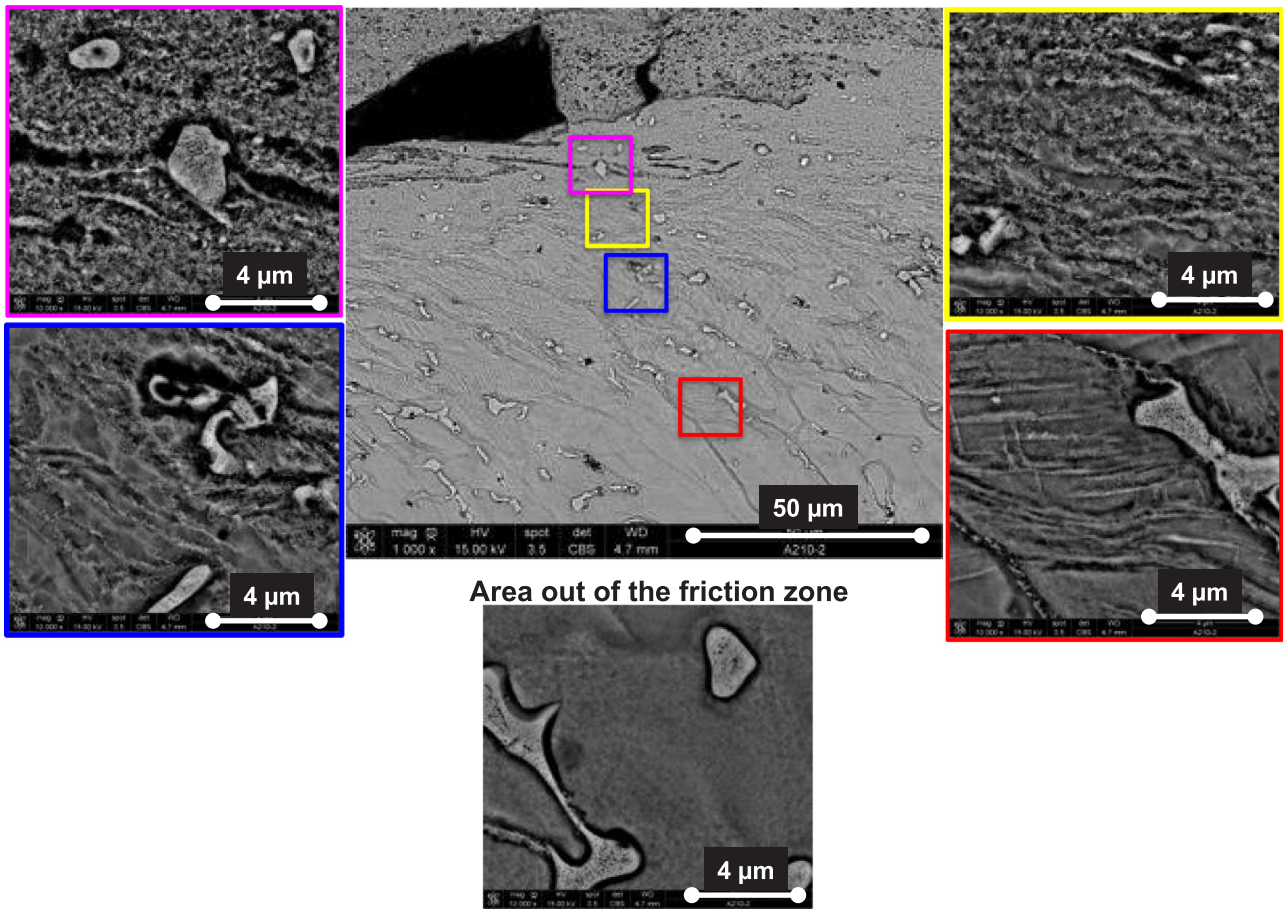

Fig. 14. SEM observations of recrystallization mechanism in the upper layers of the TTS under very severe tribological conditions (MIG coating).

3.2. Identification of some mechanisms of plasticity supported by the Mode M3 (shear Mode)

3.2.1. Mechanisms of plasticity described by a dual-tempered martensitic steel

The TTS, in this grade of steel (X38CrMoV5 steel) and under the tribological conditions used (Table 1), correspond to highly plastically sheared areas (the term of super-ductility could be used to describe it). It is made possible because of very high plastic strain without hardening, without recrystallization but certainly with softening of the martensitic laths. Thus, a physical definition of Shear Mode M3, given previously, could be assessed as a softening of the martensitic structure. The softening or deconsolidation of the upper layers of the TTS was supported by hardness measurements. The measurements (Fig. 2) showed a decrease in the pin-surface hardness which indicates the softening of the TTS under the effect of "cyclic" stresses caused by the intense friction shearing. This softening or deconsolidation is also supported by TEM observations. Using the FIB method (Focused Ion Beam) to prepare ultra-thin TEM samples, the extreme surface of a X38CrMoV5 steel pin was observed by TEM over a depth of 5 µm. Because of its thermal treatment (quenching and tempering), the density of dislocations in the dual-tempered martensitic steel X38CrMoV5 is initially very high (Fig. 10-a). By moving upwards to the surface, Fig. 10-b and c show that friction stresses tend to decrease the dislocation density continuously by dynamic recovery, characterized by the annihilation of dislocations and the development of a band-like arrangement consisting of grains and sub-grains aligned parallel to the sliding direction. This feature (dynamic recovery) could then explain the intense plastic deformations as well as softening (Fig. 10). This means that under our conditions, the extreme surface is able to deform to very large deformations without dynamic recrystallization since the TEM micrographs always show the presence of the laths. This softening or deconsolidation is also supported by the understanding of the fatigue behavior of this steel. It is known to have a strong sensitivity to the Rochet effect, which implies the notion of cycle with the possibility of a plastic strain increment at each deformation cycle (ratcheting). The deconsolidation then makes it possible to achieve a high ductility such as that measured in torsion tests (shear strain > 700%). Then, because of the fatigue behavior outlined previously, it is considered that when the cumulative shear plastic strain at the sub-surface reaches the critical strain limit (shear rupture ductility), a small number of laths are locally ruptured, forming the inter-lamellar micro-cavities. These micro-cavities coalesce and form sharp micro-cracks that propagate under shear stresses (M3 mode). This propagation is along the sliding direction and mostly takes place in an inter-lath manner, which eventually leads to wear-particle emission. The softening phenomenon under friction stresses explains the shape of the wear particle. Thus, a physical definition of the Mode M2, given previously for achieving the metallic wear particle, can also be assessed.

3.2.2. Mechanisms of plasticity described by the cobalt-base alloy (Stellite 21 coating)

Under the tribological parameters close to industrial forging conditions (Table 2), post mortem XRD analyses and EBSD measurements on TTS of the MIG process coatings revealed that the Co remains Face-Centered Cubic (FCC) (Fig. 11-a and b) while it becomes HCP for the LASER process coating TTS (Fig. 11-a and b). The microstructure of the TTS of the MIG coatings remains (FCC), because of the high iron content (> 35% in mass). Thus, the shear mode M3 only results from plastic deformation mechanisms by strain hardening. It involves the

sliding of perfect dislocations and their entanglements by their interactions. The dislocation density therefore increases with plastic deformation due to their multiplication, and leads to hardening. The sliding of perfect dislocations is also one of the mechanisms leading to the crystallographic texturing of the surface. In the case of a MIG coating TTS, which does not change its phase under tribological solicitations, STEM images reveal a large amount of entangled dislocations and only a few stacking defects in the upper layers of the TTS (Fig. 12). This type of deformation mechanism results in a relative hardening rate (strain-hardening) of around 85% in the upper layers of the TTS.

In the TTS of the LASER process coating, an additional plastic deformation mechanism superimposes on the previous one. In addition to the plastic deformation mechanism by dislocation sliding, plastic deformation also occurs by the transformation of the metastable FCC phase into a stable HCP. This mechanism is promoted because of a much lower iron dilution inside the coating during the process (lower input energy). In these upper layers, STEM images highlight a large amount of stacking defects (black stripes) and very few dislocations (Fig. 13). Dislocation entanglement is no longer observed, as it was in the previous case. In the upper layers of the TTS, the shear mode M3 is the result of a mix of these two plastic deformation mechanisms. Such deformation mechanisms result in strain hardening around 50%. In the lowest layers of the TTS, the microstructure remains FCC and the relative hardening rate is around 35%. The accommodation mechanism of the plastic deformation by phase transformation seems to be possible only from a certain level of strain hardening. When this rate is reached, the transformation would then be progressive and not instantaneous. One could assume that when phase transformation is in action, the rearrangement of the dislocations occurs.

Another finding of these studies is that recrystallization of the TTS might occur in the first layers of the TTS (Fig. 14) if the tribological parameters are too severe. In Fig. 14, a gradient of plastic-deformation mechanisms can be observed from the surface towards the sub-layers of the TTS. Because of the very severe tribological parameters, recrystallization in extreme surfaces seems to occur, then areas of large plastic deformation with the presence of stacking faults are observed, whilst outside of the friction zone, almost no stacking faults can be distinguished.

For cobalt-alloy coating and depending on the process used, the M3 mode in the TTS (S1M3) can be supported by different physical mechanisms of plasticity, such as strain-hardening, martensitic transformation and even recrystallization.

4. Conclusion

This article summarizes several tribological investigations on two different alloy grades. After friction experiments, an area with a plastic flow greater than a few hundred percent was identified at the extreme surface of the friction contact. This was the case regardless of whether it was a dual-tempered martensitic steel or a cobalt-base alloy coating. This area is related to Tribologically Transformed Surfaces (TTS) or Superficial Tribological Transformations (STT). In our investigations, these layers result from changes in microstructural, mechanical and, doubtless, in thermal properties but not from chemical modifications.

Thus, according to the parameters directly related to the metallurgy of the samples under frictional stresses, the accommodation of shear mode M3 in these TTS is supported by several mechanisms of plasticity, such as softening, strain-hardening, phase transformation and recrystallization.

Depending on the thickness affected by the tribological transformations, these mechanisms can be combined or not. These mechanisms lead to very drastic plastic deformations, which certainly result from the mechanical action of high hydrostatic pressures and cyclic shear plastic accumulations under friction stresses, even under low temperature conditions.

References

[1] A. Eleöd, F. Oucherif, J. Devecz, Y. Berthier, Conception of numerical and experimental tools for study of the tribological transformation of surface (TTS), in: D. Dowson (Ed.), Lubrication at the Frontier, 1999, pp. 673–682.
[2] Y. Berthier, Third-Body reality - Consequences and use of the Third-Body Concept to solve friction and wear problems, in: G. Stachowiak (Ed.), Wear & Materials, Mechanisms and Practice, 2005 (Chapter 12).
[3] S. Descartes, M. Busquet, Y. Berthier, An attempt to produce ex situ TTS to understand their mechanical formation conditions - The case of an ultra high purity iron, Wear 271 (2011) 1833–1841.
[4] G. Antoni, T. Désoyer, F. Lebon, Tribological transformation of surface: a thermo-mechanical modelling, in: Proceedings of the 10th International Conference in Computational Structures Technology, Vol 93, 2010.
[5] D.A. Rigney, Comments on the sliding wear of metals, Tribol. Int. 30 (5) (1997) 361–367.
[6] A. Kapoor, F.J. Franklin, Tribological layers and the wear of ductile materials, Wear 245 (2000) 204–215.
[7] J.L. Young Jr., D. Kuhlmann-Wilsdorf, R. Hull, The generation of mechanically mixed layers (MMLs) during sliding contact and the effects of lubricant thereon, Wear 246 (2000) 74–90.
[8] S. Fouvry, T. Liskiewicz, Ph Kapsa, S. Hannel, E. Sauger, An energy description of wear mechanisms and its applications to oscillating sliding contacts, Wear 255 (2003) 287–298.
[9] D.A. Rigney, Transfer, Mixing and associated chemical and mechanical processes during the sliding of ductile materials, Wear 245 (2000) 1–9.
[10] P. Blau, Elevated-temperature tribology of metallic materials, Tribol. Int. 43 (2010) 1203–1208.
[11] S. Descartes, Y. Berthier, Rheology and flows of solid third bodies: background and application to an MoS1.6 coating, Wear 252 (2002) 546–556.
[12] N. Fillot, I. Iordanoff, Y. Berthier, Wear modeling and the third body concept, Wear 262 (2007) 949–957.
[13] J. Denape, Third Body Concept and Wear Particle Behavior in Dry Friction Sliding Conditions, Trans. Tech. Publications, 2014, pp. 1–12.
[14] Y. Berthier et al. Vers une conception de matériaux pour application tribologique, Colloque Matériaux 2002: de la conception à la mise en oeuvre, Oct 2002, France 2002.
[15] V. Linck, L. Baillet, Y. Berthier, Modeling the consequences of local kinematics of the first body on friction and on third body sources in wear, Wear 255 (2003) 299–308.
[16] N.P. Suh, An overview of the delamination theory of wear, Wear 44 (1977) 1–16.
[17] W.M. Rainforth, Microstructural evolution at the worn surface: a comparison of metals and ceramics, Wear 245 (2000) 162–177.
[18] B. Bhushan, M. Nosonovsky, Scale effects in friction using strain gradient plasticity and dislocation-assisted sliding (microslip), Acta Mater. 51 (2003) 4331–4345.
[19] P.L. Menezes, Kishore, S.V. Kailas, Role of surface texture of harder surface on subsurface deformation, Wear 266 (2009) 103–109.
[20] L. Meshi, S. Samuha, S.R. Cohen, A. Laikhtman, A. Moshkovich, V. Perfilyev, I. Lapsker, L. Rapoport, Dislocation structure and hardness of surface layers under friction of copper in different lubricant conditions, Acta Mater. 59 (2011) 342–348.
[21] S. Fayeulle, P. Blanchard, L. Vincent, Fretting behavior of titanium-alloys, Tribol. Trans. 36 (2) (1993) 267–275.
[22] T. Hisakado, K. Akiyama, K. Matsuzawa, H. Ishigaki, Wear mechanism of stainless steel confirmed by applications of phase-transformation of itself and CCD camera, Wear 238 (2000) 168–173.
[23] M. Zandrahimi, M. Reza Bateni, A. Poladi, J.A. Szpunar, The formation of martensite during wear of AISI 304 stainless steel, Wear 263 (2007) 674–678.
[24] M.C.M. Farias, R.M. Souza, A. Sinatora, D.K. Tanaka, The influence of applied load, sliding velocity and martensitic transformation on the unlubricated sliding wear of austenitic stainless steels, Wear 263 (2007) 773–781.
[25] Z.N. Farhat, C. Zhang, The role of reversible martensitic transformation in the wear process of TiNi shape memory alloy, Tribol. Trans. 53 (6) (2010) 917–926.
[26] U. Cihak-Bayr, G. Mozdzen, E. Badisch, A. Merstallinger, H. Winkelmann, High plastically deformed sub-surface tribozones in sliding experiments, Wear 309 (2014) 11–20.
[27] K.C. Antony, Wear resistant cobalt-base alloys, J. Metal. (1983) 52–60.
[28] A.S. D'Oliveira, P.S. Da Silva, R. Vilar, Microstructural features of consecutive layers of stellite 6 deposited by laser cladding, Surf. Coat. Technol. 153 (2002) 203–209.
[29] L. Fouilland, M. El Mansori, A. Massaq, Friction-induced work hardening of cobalt-based hardfacing deposits for hot forging tools, J. Mater. Process. Technol. 209 (2009) 3366–3373.
[30] E. Cabrol, C. Boher, V. Vidal, F. Rézaï-Aria, F. Touratier, Plastic straining of cobalt-based hardfacings under friction loading, Wear 330–331 (2015) 354–363.
[31] E.K. Ohriner, T. Wada, E.P. Whelan, H. Ocken, The chemistry and structure of wear-resistant, iron-base hardfacing alloys, Metall. Trans. A 22A (1991) 983–991.
[32] O. Barrau, C. Boher, R. Gras, F. Rezai-Aria, Analysis of the friction and wear behaviour of hot work tool steel for forging, Wear 255 (2003) 1444–1454.
[33] O. Barrau, C. Boher, R. Gras, F. Rezai-Aria, Wear mechanisms and wear rate in a high temperature dry friction of AISI H11 tool steel: influence of debris circulation, Wear 263 (2007) 160–168.
[34] C. Boher, O. Barrau, R. Gras, F. Rezai-Aria, A wear model based on cumulative cyclic plastic straining, Wear 267 (Issues 5–8) (2009) 1087–1094.
[35] P. Lepesant, C. Boher, Y. Berthier, F. Rezai-Aria, A phenomenological model of the third body particles circulation in a high temperature contact", Wear 298 (2013)

66–79.
[36] I. Souki, D. Delagnes, P. Lours, Influence of heat treatment on the fracture toughness and crack propagation in 5% Cr martensitic steel, Procedia Eng. 10 (2011) 631–637.
[37] V. Velay, G. Bernhart, L. Penazzi, Cyclic behaviour modeling of a tempered martensitic hot work tool steel, Int. J. Plast. 22 (2006) 459–496.
[38] A.T. Alpas, H. Hu, J. Zhang, Plastic deformation and damage accumulation below the worn surfaces, Wear 162–164 (1993) 188–195.
[39] J.H. Dautzenberg, J.H. Zaat, Model of strain distribution by sliding wear, Wear 26 (1973) 105–119.